Spin dynamics of the quasi-2D Heisenberg antiferromagnet Eu_2CuO_4

E. I. Golovenchits, S. L. Ginzburg,[*] V. A. Sanina, and A. V. Babinskiĭ

A. F. Ioffe Physicotechnical Institute, Russian Academy of Sciences, 194021 St. Petersburg, Russia

Spectra of excitations with frequencies ω_0 have been observed in the dielectric crystal Eu_2CuO_4 over a broad temperature range, including the vicinity of the Néel point T_N, for electromagnetic waves in the microwave range. These spectra are uniform (with a wave vector $q=0$) and well-defined (with a damping $\gamma \ll \omega_0$). In the absence of a static external magnetic field, an antiferromagnetic resonance (a gap in the spectrum of excitations) is observed in a critical region in which there are 2D antiferromagnetic spin fluctuations with large correlation radii ξ in the crystal. Uniform, well-defined spin excitations can exist in quasi-2D Heisenberg antiferromagnets when there is a pronounced anisotropy ($\xi_a \ll \xi$, where ξ_a is the radius of the correlation among spins due to the anisotropy) of a certain symmetry. Some specific mechanisms for the anisotropy for Eu_2CuO_4 are discussed. A phase state diagram is constructed. © *1995 American Institute of Physics.*

1. INTRODUCTION

In this paper we examine the spin dynamics of the antiferromagnetic dielectric crystal Eu_2CuO_4 for electromagnetic waves in the microwave range. We study the temperature dependence and the frequency dependence of the dynamic magnetic and electric susceptibilities at frequencies of 10–40 GHz over the temperature range 77–350 K for various orientations of the components of the alternating electromagnetic field with respect to the crystal axes. There is no static magnetic field.

The compound Eu_2CuO_4 belongs to the class of crystals R_2CuO_4 (R is either La or one of the rare earth elements Pr, Nd, Sm, Eu, Gd), which serve as models for high T_c superconducting compounds. In addition, the dielectric crystals R_2CuO_4 are quasi-2D Heisenberg antiferromagnets whose structure is based on CuO_2 planes. The latter consist of a 2D square lattice of spins ($S=1/2$) with antiparallel nearest neighbors. The R_2CuO_4 crystals with rare earth ions have tetragonal symmetry of the type T' ($T4/mmm$) over the entire temperature range.[1] A structural phase transition occurs in La_2CuO_4, from the tetragonal (higher-temperature) phase to an orthorhombic phase.

Among the tetragonal R_2CuO_4 crystals, only Eu_2CuO_4 contains an essentially nonmagnetic ion of a rare earth element, which has essentially no influence on the magnetic properties of the CuO_2 planes of the crystal. The $^7F_0$ ground state of the Eu^{3+} ion is nonmagnetic. The first excited magnetic state, $^7F_1$, of the Eu^{3+} ion lies 300 cm^{-1} from the ground state. The subsystem of Eu^{3+} ions constitutes a Van Vleck paramagnet and has essentially no effect on the dynamic magnetic properties of the crystal.

We believe that the properties of isolated 2D CuO_2 layers are similar in many crystals of the R_2CuO_4 type.

Strong antiferromagnetic correlations in the CuO_2 planes have been seen in experiments on inelastic neutron scattering in La_2CuO_4 (Refs. 2 and 3) and $YBa_2Cu_3O_{6+\delta}$ (Refs. 4 and 5) over a broad temperature range, including $T > T_N$. The authors have interpreted these correlations as well-defined spin-wave-like excitations with a wave vector $q - Q \approx 0$, where Q is the antiferromagnetic reciprocal lattice vector.

Two-dimensional Heisenberg antiferromagnets with $S=1/2$ were studied by Chacravarty *et al.* in Ref. 6; they were also studied in Refs. 7 and 8. It was shown in Ref. 6 that 2D antiferromagnetic long-range order with $T_N=0$ can exist in isolated 2D CuO_2 layers. At $T>0$, there are antiferromagnetic, 2D, well-defined spin-wave-like excitations with a wave vector $q'=q-Q$ at $q'\xi \gg 1$, where ξ is the correlation radius of the spin fluctuations (antiferromagnetic spin-wave excitations). In the region $q'\xi \ll 1$ these excitations become purely dissipative, in accordance with general principles. In real La_2CuO_4 and $YBa_2Cu_3O_{6+\delta}$ crystals there is a quasi-2D long-range antiferromagnetic order with a finite T_N. At $T > T_N$, well-defined antiferromagnetic spin-wave excitations can exist under the condition $q'\xi \gg 1$ according to the model of Ref. 6.

In the present study, we have observed uniform, well-defined low-frequency excitations over a broad temperature range, including temperatures above T_N, in the stoichiometric dielectric crystal Eu_2CuO_4 in the absence of a static external magnetic field. The frequencies of these excitations are near 30 GHz. We assume $T_N \approx 150-160$ K for Eu_2CuO_4. Opinion is divided regarding the value of T_N for Eu_2CuO_4 [it may be either 150–160 K (Refs. 9 and 10) or 250–270 K (Refs. 11 and 12)]. However, the experimental data of the present study, like the results of Ref. 13, can be interpreted only under the assumption $T_N=150-160$ K. We will take up the question of the value of T_N for Eu_2CuO_4 in more detail later on in this paper.

The well-defined uniform spin-wave excitations which we observed are oscillations of the total moment of the antiferromagnet (ferromagnetic spin-wave excitations). As will become clear below, oscillations of the ferro- and antiferromagnetic order parameters in an antiferromagnet are related to each other and have the same excitation spectrum.

In the case $q=0$, however, in the hydrodynamic region of critical phenomena, only damped, diffuse excitations can exist.[6,14] By analogy with Ref. 14, in which the spin dynam-

ics in the critical region of dynamic scaling for 3D ferro- and antiferromagnets was discussed, we assume that the incorporation of a pronounced anisotropy (such that $a \ll \xi_a \ll \xi$, where a is the lattice constant, and ξ_a is the radius of the correlation among spins due to the anisotropy) makes possible the existence of well-defined uniform spin-wave excitation. In other words, it leads to a gap in the spectrum of spin-wave excitations. The quantity ξ depends on the temperature, so we assume that the anisotropy is strong at temperatures at which the conditions $a \ll \xi_a \ll \xi$ hold. A study of the dynamic magnetic susceptibility at frequencies close to the frequency of the gap in the spin-wave excitations yields values for the dynamic susceptibility which are considerably higher than the static susceptibility.[9] At frequencies above the value of the gap in the spin-wave excitations, and in the case of weak but nonzero damping, negative values of the real part of the susceptibility arise. Both of these features of the dynamic magnetic susceptibility are observed in our experiments when the alternating magnetic field is oriented along the c axis of the crystal ($\mathbf{h} \| \mathbf{c}$).

In addition to the dynamic magnetic susceptibility, we studied the dynamic electric susceptibility, so we were able to monitor the conductivity and dynamics of the lattice.

This paper is organized as follows: In Sec. 2 we describe the experimental apparatus and the method for determining the magnetic and electric susceptibilities. In Sec. 3 we present experimental results. In Sec. 4 we offer a theoretical analysis of the conditions under which uniform, well-defined spin-wave excitations can exist in the critical region. In Sec. 5 we construct a phase state diagram for a Eu_2CuO_4 crystal, and we interpret the experimental results. We also discuss a problem which arises in connection with an experimental determination of T_N for Eu_2CuO_4.

2. EXPERIMENTAL PROCEDURE; METHOD FOR CALCULATING THE MICROWAVE MAGNETIC AND ELECTRIC SUSCEPTIBILITIES

The frequency dependence and temperature dependence of the magnetic and electric susceptibilities were studied over the frequency range 10–42 GHz and the temperature range 77–350 K. We used a standard microwave spectrometer layout with a TE_{10p} ($p = 2$–8) transmission cavity. We measured the temperature dependence of the resonant frequency and the Q of the cavity with and without the test sample, at frequencies corresponding to the spectrum of natural modes of the cavity. The test sample was at the center of the cavity, at a position corresponding to an antinode of the magnetic field for even p or to an antinode of the electric field for odd p. In the first case we measured the magnetic susceptibility of the sample, and in the second the electric susceptibility.

Electrodynamic parameters of the sample were calculated in the quasistatic approximation by the perturbation-theory method.[15] The corresponding expressions for the magnetic and electric susceptibilities of the sample are

$$\mathrm{Re}\ \chi_s^* = -\left(8\pi\eta\ \frac{V_s}{V_c}\right)^{-1} \mathrm{Re}\ \frac{\delta\omega^*}{\omega^*}. \tag{2.1}$$

$$\mathrm{Im}\ \chi_s^* = \left(16\pi\eta\ \frac{V_s}{V_c}\right)^{-1} \mathrm{Im}\ \frac{\delta\omega^*}{\omega^*}. \tag{2.2}$$

Here χ_s^* is the complex magnetic (electric) susceptibility of the test sample. We are using Gaussian units, in which the susceptibilities are dimensionless. Here $\delta\omega^* = \omega^* - \omega_c$, where ω^* and ω_c are the complex frequencies of the cavity with and without the test sample, respectively; V_s/V_c is the ratio of the volumes of the test sample and the cavity; and the parameter η reflects the difference between the mean field in the sample and the peak value of the field for a sample of nonzero dimensions. For small offsets ($\delta\omega \ll \omega$) we have

$$\mathrm{Re}(\delta\omega^*/\omega^*) \cong \delta\omega/\omega, \tag{2.3}$$

$$\mathrm{Im}(\delta\omega^*/\omega^*) \cong \frac{1}{2}\ \delta(1/Q). \tag{2.4}$$

Here $\delta\omega = w - w_c$, $\delta Q = Q - Q_c$; ω and Q (ω_c and Q_c) are the resonant frequency and quality factor of the cavity with and without the sample, respectively.

The expressions for the parameter η for the components e_y, h_x, and h_z of the microwave field as functions of the geometric parameters of the sample and the cavity are

$$\eta(e_y) = \frac{1}{4}\left(1 + \frac{A}{a\pi}\sin\frac{\pi a}{A}\right)\left(1 - \frac{L}{pl\pi}\cos p\pi\sin\frac{p\pi l}{L}\right),$$

$$\eta(h_x) = \frac{1}{4}\left(1 + \frac{A}{a\pi}\sin\frac{\pi a}{A}\right)\left(1 + \frac{L}{pl\pi}\cos p\pi\sin\frac{p\pi l}{L}\right),$$

$$\eta(h_z) = \frac{1}{4}\left(1 - \frac{A}{a\pi}\sin\frac{\pi a}{A}\right)\left(1 - \frac{L}{pl\pi}\cos p\pi\sin\frac{p\pi l}{L}\right).$$

Here A, L and a, l are the dimensions of the cavity and the sample along the x and z axes, respectively. We used test samples with typical dimensions of $1 \times 1 \times 0.2$ mm. For such samples, at an antinode of the magnetic field, the admixture of the electric-field component at the maximum working frequency ($p = 8$) is $\langle e_y\rangle^2/\langle h_x\rangle^2 < 10^{-2}$. The same estimate applies to the admixture of the magnetic component when the sample is at an antinode of the electric field in measurements of the electric susceptibility.

The demagnetization (depolarization) (**n**) was taken into account with the help of the formulas for an ellipsoid of revolution.[16] In this case (depolarization), the formulas for the susceptibilities are

$$\mathrm{Re}\ \chi = \chi' = (\chi_s' - 4\pi n\chi_s''\chi'')/(1 - 4\pi n\chi_s'), \tag{2.5}$$

$$\mathrm{Im}\ \chi = \chi'' = (\chi_s'' + 4\pi n\chi_s''\chi')/(1 - 4\pi n\chi_s'). \tag{2.6}$$

The measurement apparatus was calibrated with the help of a standard polycrystalline Al_2O_3 sample, whose electric susceptibility had been measured previously by the dielectric-cavity method. The different between the values of the electric susceptibility found by this method and those calculated from expressions (2.5) and (2.6) on the basis of measurements of the parameters of the cavity in our method did not exceed 10%.
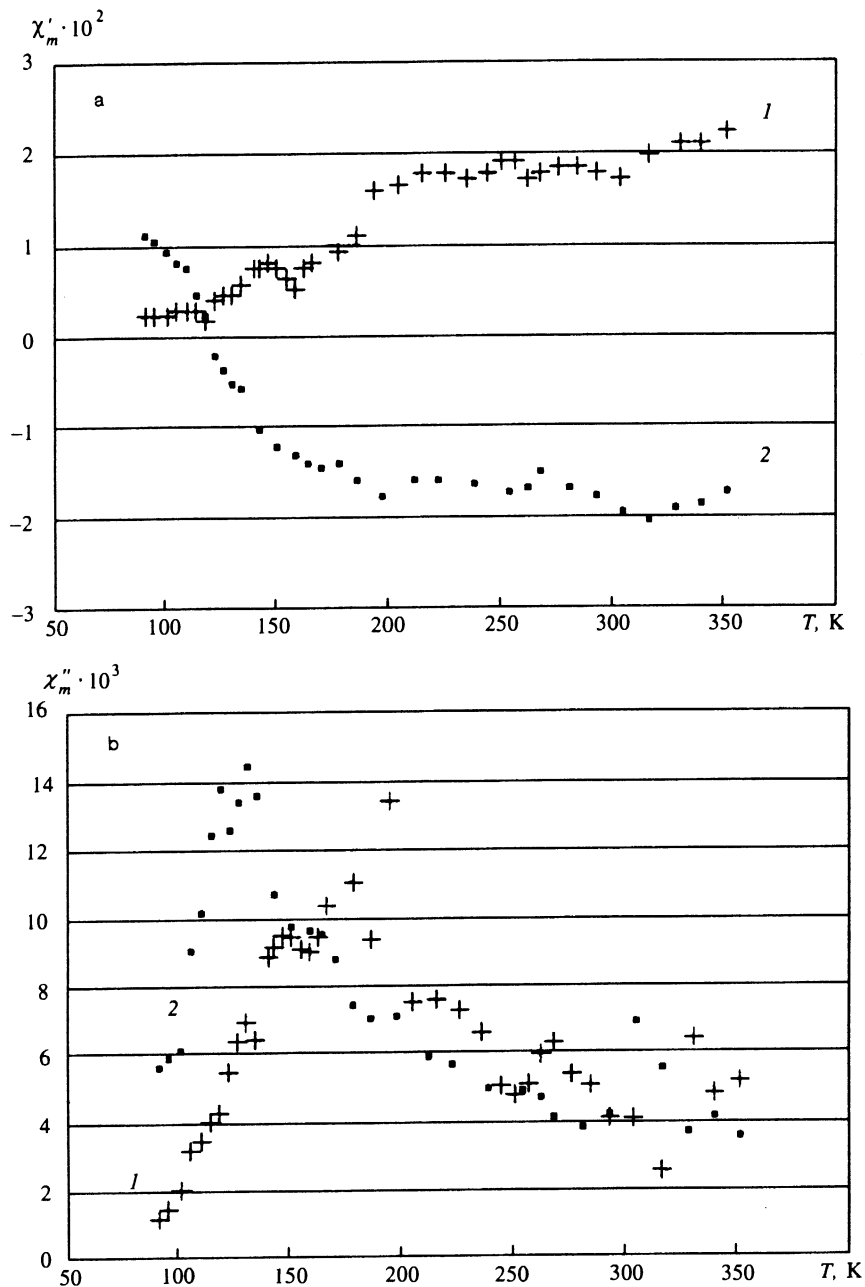
FIG. 1. Temperature dependence of the real (a) and imaginary (b) parts of the dynamic magnetic susceptibility at a frequency of 30 GHz, for two orientations of the alternating magnetic field: $h\perp c$ (curve *1*) and $h\|c$ (curve *2*).

3. EXPERIMENTAL RESULTS

Figure 1 shows the temperature dependence of the real (χ'_m) and imaginary (χ''_m) parts of the dynamic magnetic susceptibility. There is no static external magnetic field.

We first note that the values of the dynamic susceptibility from these measurements are two orders of magnitude greater than the static magnetic susceptibility for Eu_2CuO_4, for both orientations of the alternating magnetic field (Ref. 9).

We see in Fig. 1 that in the orientation $h\|c$ (curves *2*) there is a sharp change in χ'_{mc}, including a change in its sign, at $T\approx 120$ K, accompanied by a maximum in χ''_{mc}. As the temperature is raised further, χ'_{mc} remains negative and depends weakly on the temperature up to the highest temperature in these measurements, $T=350$ K. In the tempera-

ture region beyond the maximum of χ''_{mc} we have a ratio $\chi''_{mc}/\chi'_{mc} \approx 0.2$.

For the orientation $h\perp c$ (curves *1*), we see no anomalies in the temperature dependence of χ_{mpl} at $T\approx 120$ K. At $T\approx 150$ K, there are maxima in χ'_{mpl} and χ''_{mpl}. At 190–200 K there are anomalies in both the real and imaginary parts of the planar dynamic susceptibility. With a further increase in the temperature (at $T>200$ K), χ'_{mpl} also becomes independent of the temperature, remaining positive. In this temperature region, the values of χ'_{mc} and χ'_{mpl} (the difference in sign is being taken into account here) and those of χ''_{mc} and χ''_{mpl} are essentially the same.

Over a broad temperature region including $T>T_N$, there thus exist magnetic excitations for which the real parts of the dynamic magnetic susceptibility are significantly larger than
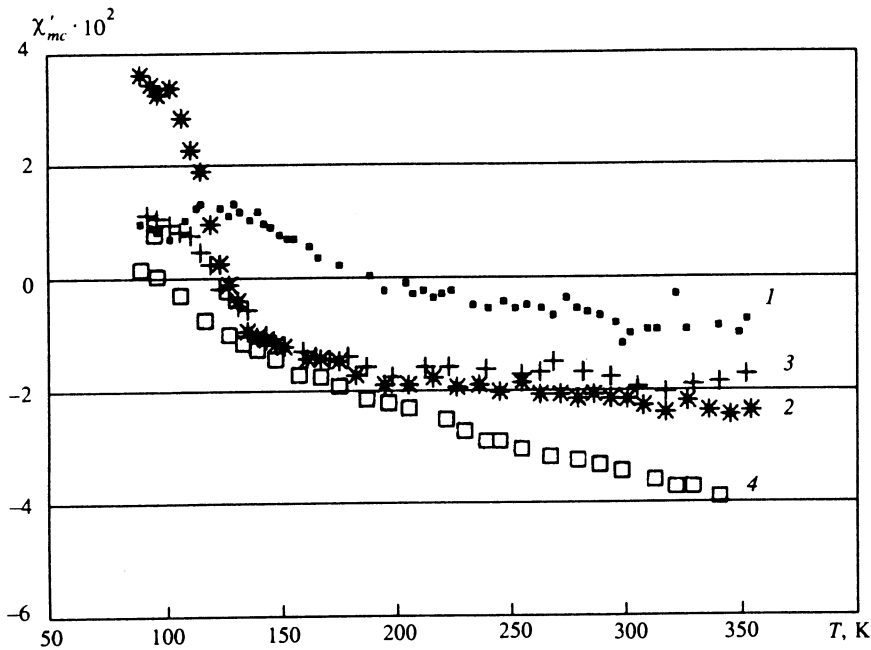
FIG. 2. Temperature dependence of the real part of the dynamic magnetic susceptibility for the orientation $h\|c$ at several frequencies in the 8-mm microwave range. 1—26 GHz; 2—30 GHz; 3—36 GHz; 4—42 GHz.

the imaginary parts of the dynamic magnetic susceptibility, and also significantly larger than the corresponding static magnetic susceptibilities.[9] At $T>T_N$ we are probably dealing with well-defined natural modes of magnetic excitations with $q=0$—an analog of an antiferromagnetic resonance at $T<T_N$. The induction of antiferromagnetic long-range order by a static external magnetic field H_0 has been observed previously[17] at $T>T_N$. In our own case we have $H_0=0$.

We carried out a frequency study of the dynamic magnetic susceptibility in the 3-cm and 8-mm microwave ranges. It turned out that the measured values of $\delta\omega/\omega$ at 10 GHz are considerably smaller than in the 8-mm range (for a given sensitivity of the spectrometer) and do not exceed the measurement errors. The corresponding values of χ'_m are less than 10^{-3}, and we assume that there are no high-Q magnetic excitations at 10 GHz.

Figure 2 shows the temperature dependence of χ'_{mc} for several frequencies in the 8-mm range. We see that the abrupt onset of negative values of χ'_{mc} at $T\approx120$ K depends on the frequency. As we have already mentioned, there is essentially no abrupt change of this sort at the frequency of 10 GHz. At 26 GHz (curve 1 in Fig. 2) the value of χ'_{mc} is considerably smaller than at higher frequencies, and it goes negative at a higher temperature. Nevertheless, we observe a maximum near $T\approx120$ K again at this frequency. We did not observe an effect of a static external magnetic field $H_0\leq1.5$ T (applied either along the c axis or in the CuO_2 plane) on the dynamic magnetic susceptibility at room temperature.

Figure 3 shows the temperature dependence of the real and imaginary parts of the electric susceptibility at a frequency of 33 GHz for two orientations of the alternating electric field: along the c axis and in the ab plane. We did not observe a frequency dependence of the electric susceptibility over the frequency range 23–40 GHz. It can be seen from Fig. 3 that in the case $e\perp c$ there is a jump in χ'_{epl} at $T\approx120$ K, accompanied by a maximum in χ''_{epl} at the same

temperature. A slight anomaly is also observed at $T\approx270$ K in the behavior of χ'_{epl}. Beginning at $T\approx270$ K, the quantity χ''_{epl} increases. For the orientation $e\|c$ up to $T\approx270$ K, both χ'_{ec} and χ''_{ec} are essentially independent of the temperature. Again, there are no structural features at $T\approx120$ K. At $T>270$ K, both the imaginary and real parts of χ_{ec} begin to increase.

Anomalies in the electric susceptibility similar to those observed here in $\chi_{epl}(T)$ at $T\approx120$ K are characteristic of structural phase transitions in crystals.

The dielectric constant of the Eu_2CuO_4 crystal also depends weakly on the temperature over the temperature range in which a uniform magnetic-resonance mode exists; it is characterized by values $\varepsilon'_{epl} = 1 + 4\pi\chi'_{ep} = 5.4$ and $\varepsilon''_{epl}=4\pi\chi''_{epl}=0.5$ in the plane perpendicular to c and by values $\varepsilon'_{ec} = 2.2$, and $\varepsilon''_{ec} = 0.1$ for the c axis.

The negative value of χ'_{mc} which we observed cannot be attributed to a trivial effect of the conductivity—to currents induced in the ab plane by an alternating field $h\|c$. That interpretation is unlikely since, if we adopt the hypothesis that χ'_{mc} is inductive, it becomes difficult to explain the frequency-selective nature of χ'_{mc} in the narrow frequency interval in which we are working. It is also difficult to understand why χ'_{mpl} would be positive, close in value to χ'_{mc}, for the orientation $h\perp c$. We will nevertheless estimate the inductive contribution to the susceptibility for our case. According to Ref. 16, the inductive susceptibility of a conducting cylinder in the field of an electromagnetic wave, for the case in which the magnetic field is parallel to the axis of the cylinder, is

$$\chi'_{ind}=-(1/48\pi)(R/\delta)^4. \tag{3.1}$$

Here R is the radius of the cylinder, σ is the conductivity, and $\delta = c/\sqrt{2\pi\sigma\omega}$ is the skin depth. Expression (3.1) incorporates the relation $R\ll\delta$, which clearly holds in our case.
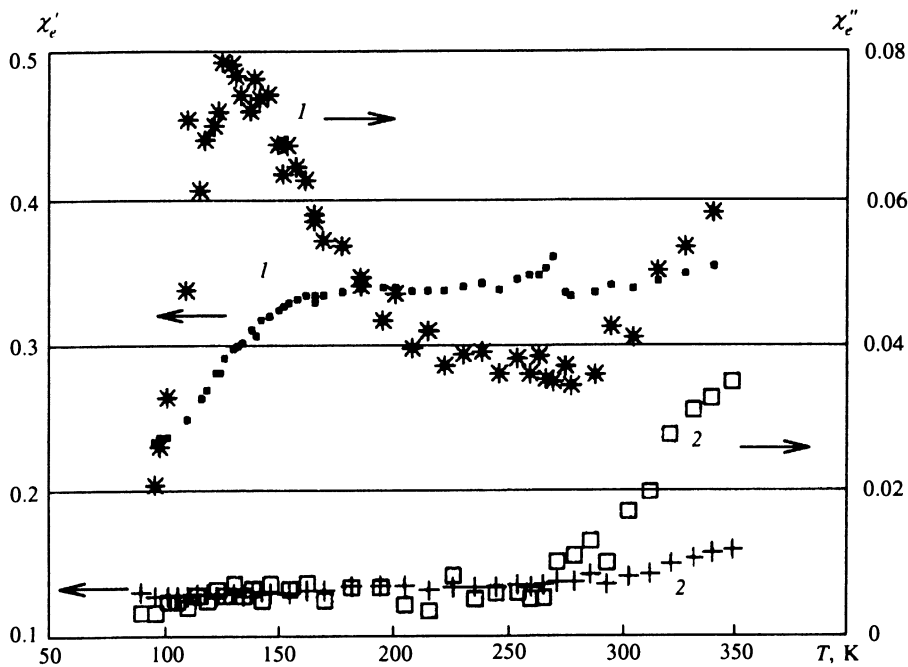
FIG. 3. Temperature dependence of the real and imaginary parts of the electric susceptibility at 33 GHz. *1*—The orientation of the alternating electric field is e⊥c; *2*—e∥c.

Assuming that dielectric losses are due entirely to conductivity $\varepsilon''=4\pi\sigma/\omega$, and using $R\approx 5\cdot 10^{-2}$ cm and $\varepsilon''=6\cdot 10^{-2}$, we find $\chi'_{\text{ind}}\approx 6\cdot 10^{-4}$, i.e., a value much lower than the experimental value.

In a dielectric crystal, the reason for the onset of a negative real part of the dynamic magnetic susceptibility may be dispersion near resonant absorption. We know that the incorporation of a small but nonzero damping near resonant absorption leads to the onset of a fairly broad frequency region $(\omega>\omega_0)$ in which the magnetic susceptibility has a negative real part. An empirical formula for the dynamic correlation function $G(\omega,\gamma)$, with two poles $(\omega=\pm\omega_0)$ and damping γ, is

$$G(\omega,\gamma)=\frac{\omega+i\gamma_0}{\omega+i\gamma+\omega_0}+\frac{i\gamma-\omega_0}{\omega+i\gamma-\omega_0},$$

$$\text{Im } G=\alpha x\left[\frac{1}{(x+1)^2+\alpha^2}+\frac{1}{(x-1)^2+\alpha^2}\right], \qquad (3.2)$$

$$\text{Re } G=\frac{x+1+\alpha^2}{(x+1)^2+\alpha^2}+\frac{1-x+\alpha^2}{(x-1)^2+\alpha^2}.$$

Here $x=\omega/\omega_0$ and $\alpha=\gamma/\omega_0$.

Figure 4 shows calculated values of Im G and Re G versus the frequency x as the damping α is varied ($\alpha=0$, 0.1,
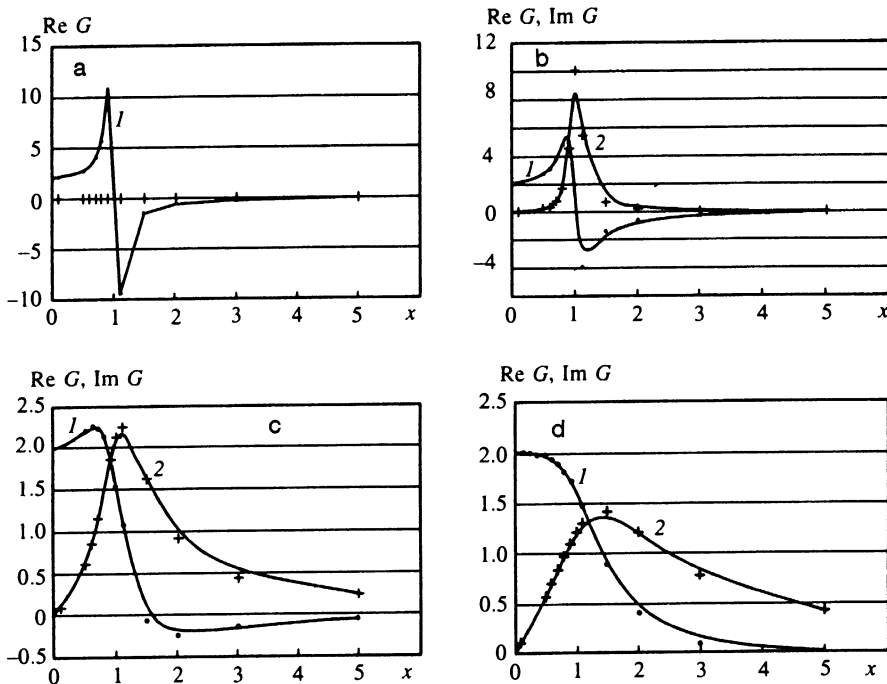

FIG. 4. Frequency dependence ($x=\omega/\omega_0$) of the real (curves *1*) and imaginary (curves *2*) parts of the dynamic correlation function $G(\omega,\gamma)$ for various values of the damping parameter $\alpha=\gamma/\omega_0$: a—$\alpha=0$; b—$\alpha=0.1$; c—$\alpha=0.5$; d—$\alpha=1$.

0.5, and 1). In the case $\alpha=0$, the imaginary part of G is described by a δ-function (at $x=1$); at nonzero values of α, the δ-function spreads out, and the nature of the dispersion of Re G changes. At a small value of α, the frequency range $\omega/\omega_0 > 1$ in which G has a negative real part becomes broader than in the $\alpha=0$ case. On the other hand, as α increases, approaching unity Re G becomes positive over the entire frequency range. The quantity Re G is always positive as $\omega/\omega_0 \to 1$ for arbitrary values $\alpha>0$. We have discussed the pole singularity for the correlation function G. In principle, however, there could be singularities of other types, e.g., branch points.

Analysis of these experimental data thus leads us to conclude that uniform $(q=0)$, well-defined spin-wave excitations with a negative value of χ'_{mc} exist in the dielectric crystal Eu_2CuO_4 over a broad temperature range $T \geqslant 120$ K, including the range $T>T_N$, for the orientation $\mathbf{h}\|\mathbf{c}$. These excitations arise abruptly at $T \approx 120$ K and then remain independent of the temperature up to $T \approx 350$ K (the measurement limit). At $T \approx 120$ K, we find anomalies in the real and imaginary parts of the electric susceptibility (for $\mathbf{e}\perp\mathbf{c}$), which are characteristic of structural phase transitions.

In the case $\mathbf{h}\perp\mathbf{c}$ at $T \geqslant 200$ K we observe a positive value of χ'_{mpl}, which depends weakly on the temperature and which is close in magnitude to χ'_{mc}. At $T \approx 150$ K there are maxima in the quantities χ'_{mpl} and χ''_{mpl}.

4. THEORETICAL ANALYSIS OF EXISTENCE CONDITIONS FOR WELL-DEFINED SPIN-WAVE EXCITATIONS IN AN ANTIFERROMAGNET IN THE CRITICAL REGION

In this section of the paper we discuss the existence of well-defined spin-wave excitations in an antiferromagnet in the critical region. For a 2D Heisenberg antiferromagnet with $S=1/2$, the concept of well-defined antiferromagnetic spin-wave excitations was introduced in Ref. 6, and the spectrum of excitations and the damping for them were discussed. The critical dynamics of a 3D antiferromagnet was studied in Ref. 14.

Only antiferromagnetic spin-wave excitations were discussed in Refs. 6 and 14. Since we measured oscillations of the total moment, we are interested in the possible existence of well-defined ferromagnetic spin-wave excitations, including some with $q=0$. In this section of the paper we examine well-defined ferro- and antiferromagnetic spin-wave excitations with $q=0$ for 3D and 2D Heisenberg antiferromagnets. By analogy with Ref. 14, we assume that spin-wave excitations of this sort can exist in the critical region when there is a pronounced anisotropy of a certain symmetry.

Let us outline this section of the paper. We first consider a 3D Heisenberg antiferromagnet in the exchange approximation at low temperatures; we write ferro- and antiferromagnetic dynamic magnetic susceptibilities and the natural frequencies of excitation. We introduce some definitions, and we examine the conditions for the existence of well-defined ferro- and antiferromagnetic spin-wave excitations in the critical region. We then show that incorporating a pronounced anisotropy of a certain symmetry makes possible the existence of well-defined uniform ferro- and antiferromagnetic spin-wave excitations in the critical region.

A corresponding procedure will be carried out for a 2D Heisenberg antiferromagnet at $T>0$.

4.1. Three-dimensional Heisenberg antiferromagnet

Exchange approximation

We first consider a 3D Heisenberg antiferromagnet with the Hamiltonian

$$H = \sum_{ij} J\mathbf{S}_i\mathbf{S}_j. \tag{4.1}$$

We assume that the exchange integral J is zero except for nearest neighbors. We assume that there is a simple cubic lattice and *staggered magnetization*. For an antiferromagnet it is convenient to introduce two sublattices (A and B) and to define spin operators in terms of Bose operators for the two sublattices in different ways (Ref. 8, for example). For sublattice A we have

$$S_i^+ = a_i\sqrt{2S}, \quad S_i^- = a_i^+\sqrt{2S}, \quad S_i^z = S - a_i^+ a_i. \tag{4.2}$$

For sublattice B we have

$$S_i^+ = b_i^+\sqrt{2S}, \quad S_i^- = b_i\sqrt{2S}, \quad S_i^z = -S + b_i^+ b_i. \tag{4.3}$$

Equations (4.2) and (4.3) hold at low temperatures. Hamiltonian (4.1) takes the following form in terms of Bose operators in the q representation:

$$H = SJ(0)\sum_q [a^+(\mathbf{q})a(\mathbf{q}) + b^+(\mathbf{q})b(\mathbf{q})]$$

$$+ SJ(\mathbf{q})\sum_q [a^+(\mathbf{q})b^+(\mathbf{q}) + a(\mathbf{q})b(\mathbf{q})],$$

$$a(\mathbf{q}) = \sqrt{\frac{2}{N}} \sum_{i\in A} \exp(i\mathbf{q}\mathbf{r}_i)a_i, \tag{4.4}$$

$$b(\mathbf{q}) = \sqrt{\frac{2}{N}} \sum_{i\in B} \exp(-i\mathbf{q}\mathbf{r}_i)b_i.$$

We define the ferromagnetic $(D_M = -\chi_M)$ and antiferromagnetic $(D_N = -\chi_N)$ susceptibilities as follows:

$$D_M(\mathbf{q},t) = -i/4\langle[S_A^-(\mathbf{q},t) + S_B^-(\mathbf{q},t);S_A^+(\mathbf{q},0)$$

$$+ S_B^+(\mathbf{q},0)]\rangle\theta(t), \tag{4.5}$$

$$D_N(\mathbf{q},t) = -i\langle[S_A^-(\mathbf{q},t) - S_B^-(\mathbf{q},t);S_A^+(\mathbf{q},0)$$

$$+ S_B^+(\mathbf{q},0)]\rangle\theta(t), \tag{4.6}$$

with $\theta(t)=1$ for $t>0$ and $\theta(t)=0$ for $t<0$. Here the [...] denote a commutator. From (4.2)–(4.6) we easily find the following expressions for $D_{M,N}(\mathbf{q},\omega)$ in the ω representation:

$$D_M(\mathbf{q},\omega) = \frac{S^2[J(0)-J(\mathbf{q})]}{\omega^2-\omega_q^2},$$

$$D_N(\mathbf{q},\omega) = \frac{4S^2[J(0)+J(\mathbf{q})]}{\omega^2-\omega_q^2}, \tag{4.7}$$

$$\omega \propto -iq_a^{3/2} \qquad \omega \propto -i(q')^{3/2} \qquad \begin{array}{c}\gamma \ll \omega \\ \omega \propto (q')^{3/2}\end{array}$$

$$\gamma \propto \kappa^{3/2} \qquad\qquad \gamma \propto \kappa^{3/2} \qquad\qquad \gamma \propto \kappa^{3/2}$$

```
0                q_a              κ              q'
```

$$\begin{array}{c}\gamma \ll \omega \\ \omega \propto q_a^{3/2}\end{array} \qquad \begin{array}{c}\gamma \ll \omega \\ \omega \propto q_a^{3/2}\end{array} \qquad \begin{array}{c}\gamma \ll \omega \\ \omega \propto (q')^{3/2}\end{array}$$

$$\gamma \propto \kappa^{3/2} \qquad\qquad \gamma \propto \kappa^{3/2} \qquad\qquad \gamma \propto \kappa^{3/2}$$

```
0        κ                      q_a             q'
```
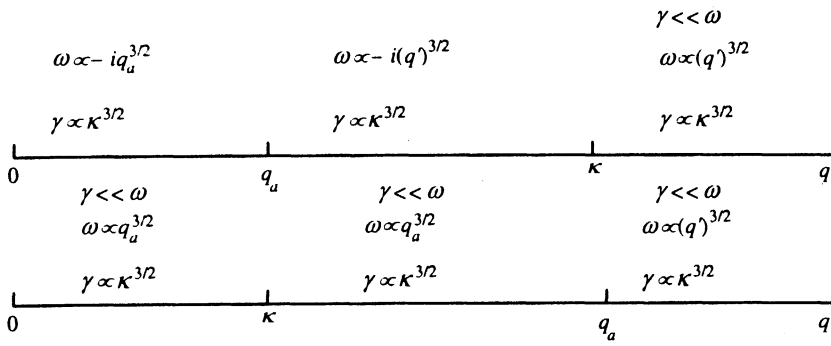
FIG. 5. Schematic diagram of the natural frequencies of spin-wave excitations in the critical region as a function of the quantity q', for various relations among q', q_a, and κ. See the text proper for an explanation.

$$D_M(\mathbf{q},0)=-\frac{1}{J(0)+J(\mathbf{q})}, \qquad D_N(\mathbf{q},0)=-\frac{1}{J(0)-J(\mathbf{q})} \tag{4.8}$$

$$\omega_q^2=S^2[J(0)^2-J(\mathbf{q})^2] \tag{4.9}$$

$$J(\mathbf{q})=J(\cos q_x a+\cos q_y a+\cos q_z a). \tag{4.10}$$

Let us discuss these expressions. First, we see from (4.7) that both susceptibilities (D_M and D_N) have singularities in the case $\omega=0$ at two points in the Brillouin zone: at $q=0$ and $\mathbf{q}=\mathbf{Q}$, where $\mathbf{Q}=(\pi/a,\pi/a,\pi/a)$ is the antiferromagnetic vector of the reciprocal lattice. The singularity in the expression for D_M at $q=0$ corresponds to oscillations of the total moment of the antiferromagnet; that at $\mathbf{q}=\mathbf{Q}$ corresponds to oscillations of the antiferromagnetic vector. The structure of the singularities in the expression for D_N is just the opposite: the singularity at $q=0$ corresponds to oscillations of the antiferromagnetic vector, and that at $\mathbf{q}=\mathbf{Q}$ corresponds to oscillations of the total moment of the antiferromagnet. Only the correlation function D_N was discussed in Ref. 14, so our region of small values of q' (more on this below) corresponds to their region of small values of q.[14] That these types of oscillations differ in nature can be seen from the expressions for the static susceptibilities. The expression for D_M has a singularity at $\mathbf{q}=\mathbf{Q}$, and that for D_N has one at $q=0$. In the dynamic susceptibilities, the residue in the expression for D_M vanishes at $q=0$, and that in D_N vanishes at $\mathbf{q}=\mathbf{Q}$. The reason why the singularities are of this nature is that the critical order parameter in an antiferromagnet is the antiferromagnetic order parameter, not the uniform magnetization.

In 3D Heisenberg antiferromagnets there are thus three types of natural excitations with frequencies (4.9). For D_M, these are oscillations of the uniform magnetization of the antiferromagnet with a wave vector $\mathbf{q}$ (ferromagnetic excitations) and oscillations of the antiferromagnetic order parameter with the wave vector $\mathbf{q}'=\mathbf{q}-\mathbf{Q}$ (antiferromagnetic excitations). In the exchange approximation, with $q,q'=0$, there are two soft modes: at the center of the Brillouin zone and at its edge. Only the antiferromagnet order parameter with the soft mode at the boundary of the Brillouin zone is critical for an antiferromagnet.

For studies of microwave absorption at natural frequencies of the antiferromagnet at $T<T_N$, one measures an antiferromagnetic resonance: the gap in the spectrum of ferro-

magnetic spin excitations with $q=0$. In neutron studies, it is customary to examine antiferromagnetic spin excitations with $q'=q-Q\to0$.

According to the results of Ref. 14, for a 3D antiferromagnet in the critical region, in the hydrodynamic approximation, i.e., with $q'a$, $\kappa a\ll1$, and under the condition $q'\gg\kappa=1/\xi$, there are well-defined antiferromagnetic spin-wave excitations with a frequency and damping

$$\omega\propto(q')^{3/2}, \qquad \gamma\propto\xi^{-3/2}, \qquad \xi\propto[|T-T_N|/T_N]^{-0.7}. \tag{4.11}$$

In the hydrodynamic region of critical phenomena, with $q'\ll\kappa$, antiferromagnetic spin-wave excitations are relaxing entities.

Let us assume that the same situation prevails for ferromagnetic spin-wave excitations, i.e., that there are well-defined ferromagnet spin-wave excitations with the frequency and damping in (4.11), with q' replaced by q, in the critical region, in the hydrodynamic approximation, and under the condition $q\gg\kappa$. In the hydrodynamic region of critical phenomena, there are only diffuse modes in the case $q\ll\kappa$.

In the exchange approximation, in the hydrodynamic region of critical phenomena, spin excitations with $q'=q=0$ are thus relaxing entities for a 3D Heisenberg antiferromagnet in the exchange approximation.

Incorporation of anisotropy

Incorporating anisotropy for a 3D Heisenberg antiferromagnet may alter the situation and make possible the existence of well-defined uniform ferro- and antiferromagnetic spin-wave excitations in the critical region. When the anisotropy in a 3D antiferromagnet in the critical region is taken into account, an additional microscopic length scale ξ_a arises (in addition to the correlation radius of the spin fluctuations in the exchange approximation ξ). This new length scale characterizes the radius of the spin correlations due to the anisotropy. According to Ref. 14 we have

$$\xi_a=a\sqrt{T_{mf}/T_a}. \tag{4.12}$$

Here a is the lattice constant, T_{mf} is the temperature characterizing the mean field (in the exchange approximation we have $T_{mf}=6JS^2$, $T_a=K_aS^2$, and K_a is the anisotropy constant.

Depending on the relations among q', κ, and $q_a=1/\xi_a$, the natural frequencies of the excitations may differ in na-

ture. These frequencies are shown in Fig. 5. In the case $q_a \ll \kappa$ (the upper diagram in Fig. 5) there are spectra of excitations in the region $q' \gg \kappa$ with a frequency $\omega \propto (q')^{3/2}$. At $q' \ll \kappa$ there are only damped modes. In the case $q_a \gg \kappa$ (the lower diagram in Fig. 5), a solution arises in the case $q' \ll \kappa$ which holds in the critical region in the case $q' \gg \kappa$; i.e., we have $\omega \propto (q')^{3/2}$, but with the replacement by $\omega \propto q_a^{3/2}$. This solution propagates into the region $q' \ll \kappa$, all the way to the point $q' = 0$, from the region $\kappa \ll q' \ll q_a$.

We assume that the same situation prevails for ferromagnetic spin-wave excitations with q' replaced by q.

If the anisotropy satisfies two conditions, then well-defined uniform ferromagnetic ($q = 0$) and antiferromagnetic ($q' = 0$) spin-wave excitations with the frequency and damping

$$\omega \propto q_a^{3/2}, \quad \gamma \propto \xi^{-3/2} \tag{4.13}$$

arise in a 3D Heisenberg antiferromagnet. These two conditions are as follows: first, the anisotropy has a symmetry which leads to a disruption of the rotational invariance of the spins that prevails in the exchange approximation (e.g., a uniaxial easy-axis anisotropy or an cubic anisotropy). Second, the anisotropy is strong enough to satisfy the conditions $a \ll \xi_a \ll \xi$ (these conditions can always be arranged sufficiently close to T_N).

In the case of a weak anisotropy, with $\xi_a \gg \xi$, the situation is the same as for an isotropic 3D Heisenberg antiferromagnet.

4.2. Two-dimensional Heisenberg antiferromagnet

Exchange approximation

Let us analyze the situation with well-defined spin-wave excitations in a 2D Heisenberg antiferromagnet with $S = 1/2$ on the basis of the model of Ref. 6, in which Hamiltonian (4.1) is considered. According to that model, a 2D Heisenberg antiferromagnet with $S = 1/2$ can have 2D antiferromagnetic long-range order at $T = 0$. At $T > 0$ there exist 2D antiferromagnetic spin fluctuations with large correlation radii ξ:

$$\xi = C_\xi a \, \exp(2\pi\rho_s/T). \tag{4.14}$$

Here $C_\xi = 0.5$ (Refs. 6 and 7), and $2\pi\rho_s$ is the spin stiffness ($2\pi\rho_s \approx 1250$ K for La_2CuO_4; Refs. 2, 3, and 6). At $T = 150$ K we have $\xi \approx 2000a$.

It was shown in Ref. 6 that an antiferromagnet with a dimensionality D ($2 < D \leq 4$) can have well-defined antiferromagnetic spin-wave excitations with a frequency and damping

$$\omega \propto (q')^{D/2}, \quad \gamma \propto \xi^{-D/2} \tag{4.15}$$

in the critical region, in the hydrodynamic approximation, in the case $q' \gg \kappa$. For a 2D Heisenberg antiferromagnet, at temperatures $T > 0$ and at q' values such that the conditions $a \ll 1/q' \ll \xi$ hold, there exist antiferromagnetic spin-wave excitations with a linear dispersion relation

$$\omega \approx \sqrt{\frac{\rho_s(1/q')}{\chi_\perp(1/q')}} \; q' = c\left(\frac{1}{q'}\right)q', \tag{4.16}$$

but the quantities $\rho_s(1/q')$, $\chi_\perp(1/q')$, and $c(1/q')$ (the spin-wave velocity) are determined on a local scale $1/q'$. In the case $q' \xi \gg 1$, these antiferromagnetic spin-wave excitations are well-defined:

$$\gamma/\omega \sim \left[\frac{1}{1 + \ln(q'\xi)}\right]^w \ll 1, \tag{4.17}$$

where w is some exponent. In the limit $q'\xi \to 1$ we have $\gamma/\omega \to 1$. The values found for γ from Eqs. (4.15) and (4.17) in the approximation $q'\xi \gg 1$ are not the same, although for both formulas $\gamma/\omega \ll 1$ at $q'\xi \gg 1$.

In the case $q'\xi \ll 1$, in the hydrodynamic region, only damped diffuse excitation spectra can exist in 2D Heisenberg antiferromagnets.[6] According to the calculations of Ref. 7, the damping of antiferromagnetic spin-wave excitations in the case $q'\xi \ll 1$ is described by $\gamma \to \gamma_0 = const$ in the limit $q' \to 0$.

We assume that the situation for ferromagnetic spin-wave excitations in 2D Heisenberg antiferromagnets is the same as for antiferromagnetic spin-wave excitations. In other words, the frequency and damping of the ferromagnetic spin-wave excitations are described by Eqs. (4.15)–(4.17), with q' replaced by q, in the critical region, in the hydrodynamic approximation, and under the condition $q \gg \kappa$. In the hydrodynamic region of critical phenomena, with $q \ll \kappa$, there are only damped modes.

Incorporation of anisotropy

Anisotropy of a 2D Heisenberg antiferromagnet was not considered in Ref. 6. Here we assume that the effect of anisotropy for a 2D Heisenberg antiferromagnet is analogous to the effect in a 3D antiferromagnet, which was studied in Ref. 14 for antiferromagnetic spin-wave excitations, and which was generalized in the preceding section of this paper to ferromagnetic spin-wave excitations. For example, we consider a uniaxial easy-axis anisotropy with a characteristic energy $T'_a = K'_a S^2$. By analogy with (4.14), the quantity ξ_a is then given by

$$\xi_a^{2D} \approx a \, \exp(2\pi\rho_s/T'_a). \tag{4.18}$$

We assume that if the anisotropy is strong enough that $a \ll \xi_a^{2D} \ll \xi$, then there can exist ferro- and antiferromagnetic spin-wave excitations with frequency (by analogy with the lower diagram in Fig. 5)

$$\omega_0 = cq_a^{(2D)}, \quad q_a^{(2D)} = 1/\xi_a^{(2D)} \tag{4.19}$$

and damping

$$\gamma = c\xi^{-1} = c\kappa. \tag{4.20}$$

Since $q_a \gg \kappa$, we have $\gamma/\omega_0 \ll 1$. In other words, ferro- and antiferromagnetic spin-wave excitations of this type are well-defined. This is the situation down to values $q, q' = 0$; i.e., this is also the situation for uniform ferro- and antiferromagnetic spin-wave excitations.

We thus assume that under the conditions $q, q' \gg \kappa$ there exist well-defined ferro- and antiferromagnetic spin-wave excitations in the critical region. The dimensionality of the antiferromagnet is not of fundamental importance, since the phenomena in 2D and 3D Heisenberg antiferromagnets are

essentially similar. However, it is far simpler to satisfy the conditions $q,q' \gg \kappa$ in 2D antiferromagnets in which there is a broad region along the temperature scale in which ξ is large. For 3D antiferromagnets, the correlation radii of the spin fluctuations are usually large only in the immediate vicinity of T_N, and an experimental study of well-defined spin-wave excitations is difficult. In their insulating phase, crystals of the type R_2CuO_4 and $YBa_2Cu_3O_{6+\delta}$, which contain antiferromagnetic 2D CuO_2 planes, present a unique opportunity for an experimental study of well-defined ferro- and antiferromagnetic spin-wave excitations at $T>T_N$. Crystals of this type are being studied quite actively in connection with the problem of high T_c superconductivity. One compound in this class is the crystal which we are studying here, Eu_2CuO_4. However, there is a problem here. The nature of the anisotropy (if sufficiently pronounced) in La_2CuO_4 and $YBa_2Cu_3O_{6+\delta}$ (in its insulating phase), both of which have an orthorhombic symmetry, allows the existence of well-defined uniform spin-wave excitations. The situation in the tetragonal Eu_2CuO_4 crystal, in contrast, with an easy-plane anisotropy, is more complicated. We will discuss the specific situation in the Eu_2CuO_4 crystal in the next section.

5. PHASE DIAGRAM OF STATES OF THE Eu_2CuO_4 CRYSTAL; INTERPRETATION OF EXPERIMENTAL DATA ON UNIFORM SPIN DYNAMICS

Proceeding in accordance with the experimental data in Sec. 3, and making use of the theoretical situation discussed in Sec. 4, we assume that uniform, well-defined, ferromagnetic spin-wave excitations arise at a temperature $T \gg 120$ K for the orientation along the c axis. We assume that these excitations exist up to high temperatures.

On the other hand, Eu_2CuO_4 is known[9,11,12] to have antiferromagnetic order at $T<T_N$; the spins lie in the xy plane. In other words, an easy-plane anisotropy is predominant in this crystal at these temperatures. As we have already mentioned, an easy-plane anisotropy cannot lead to well-defined, uniform, ferromagnetic spin-wave excitations. The fact that such spin-wave excitations arise at $T \geq 120$ K suggests that there is a change in the sign in the anisotropy at $T \approx 120$ K (easy-plane$\rightarrow$easy-axis). According to Ref. 13, it is at $T \geq 120$ K that an orbital-glass state arises in Eu_2CuO_4. It is natural to suggest that at $T \geq 120$ K the nature of the anisotropy of the spin subsystem may change, from easy-plane to easy-axis. We will adopt this assumption and attempt to reach an understanding of this situation by working from the Hamiltonian

$$H = \sum_{ij} J S_i S_j + \sum_{ik} J_\perp S_i S_k + \sum_{ij} K_a S_i^z S_j^z + \lambda \sum_i S_i^z \sigma_i^z. \quad (5.1)$$

Here we have taken into account, along with 2D Heisenberg exchange, with the constant J; an interplanar exchange with a constant $J_\perp$ (the subscripts i and k refer to nearest neighbors in adjacent planes); an easy-plane anisotropy, with a constant K_a; and a spin-orbit interaction, with a constant λ. Here σ is the projection of the orbital angular momentum of the Cu^{2+} ion.

Since the in-plane exchange and the interplanar exchange are both antiferromagnetic, the exchange constants satisfy $J>0$ and $J_\perp>0$.

In the case $S=1/2$ (Cu^{2+}), there is no single-ion anisotropy, so we have written a uniaxial ion–ion anisotropy (anisotropic exchange) in (5.1). In the case $K_a>0$ (for the selected sign of the constant J), this anisotropy is an easy-plane anisotropy.

As in Ref. 13, we adopt a degenerate tetragonal doublet $\sigma_i^z = \pm 1$ as the orbital ground state of the Cu^{2+} ions, and we assume that the spin-orbit interaction outweighs the orbit-phonon interaction.

We assume $J \gg J_\perp$, K_a, λ. In this case we have $J_\perp \sim K_a$ and $\lambda > J_\perp$, K_a. In the zeroth approximation, when we take only the 2D Heisenberg exchange into account, we have the model of Ref. 6. The effect of each of the slight interactions will be discussed independently.

When an interplanar antiferromagnetic exchange $J_\perp \sim 10^{-5} J$ is taken into account (according to Ref. 6, we have $J_\perp \ll J$ for La_2CuO_4), a quasi-2D state with a finite T_N is established in the crystal:

$$T_N \sim T_{mf}^{2D}/\ln(J/J_\perp), \quad T_{mf}^{2D} = 4JS^2. \quad (5.2)$$

If we assign Eu_2CuO_4 the same values of J and $J_\perp$ as for La_2CuO_4 (Refs. 2 and 3), specifically, $J \approx 1250$ K and $J_\perp \approx 10^{-5} J$, we find $T_N \approx 110$ K. At $T>T_N$, isotropic 2D antiferromagnetic spin fluctuations with correlation radii ξ given by (4.14) arise over a wide temperature range. The fact that $J_\perp$ is small in comparison with J has essentially no effect on the state of the 2D antiferromagnetic layers at $T>T_N$, but it does give rise to a finite T_N and to a narrow 3D antiferromagnetic critical region.[6] There have been no theoretical papers on the nature of the quasi-2D spin fluctuations for a Heisenberg antiferromagnet at $T<T_N$.

Incorporating an easy-plane anisotropy along with 2D Heisenberg exchange in isolated layers leads to a Kosterlitz–Thouless situation.[18,19] Specifically, a characteristic temperature

$$T_{KT} \approx T_{mf}^{2D}/\ln(J/K_a) \quad (5.3)$$

arises, below which there is an antiferromagnetic spin stiffness with an infinite correlation radius in the layers. At $T>T_{KT}$ there are 2D antiferromagnetic spin fluctuations with a finite correlation radius. Since we have $K_a \ll J$, at $T>T_{KT}$ a weak easy-plane anisotropy, like a slight interplanar exchange $J_\perp$, discussed above, has essentially no effect on the state of the isolated 2D layers.

A spin-orbit interaction in Eu_2CuO_4 was taken into account along with 2D Heisenberg exchange in Ref. 13. Under the assumptions adopted in Ref. 13, which are listed above, it was shown that at temperatures $T>T_N$, at which there are isotropic 2D antiferromagnetic spin fluctuations in the crystal, an orbital-glass state exists in the crystal in the case of orientation along the c axis.

As a result of the analysis of the effect of weak interactions on a 2D Heisenberg antiferromagnet with $S=1/2$ carried out above, it can be assumed that at some sufficiently high temperature $T>T_N$, T_{KT} we are dealing with isolated layers with isotropic 2D antiferromagnetic spin fluctuations
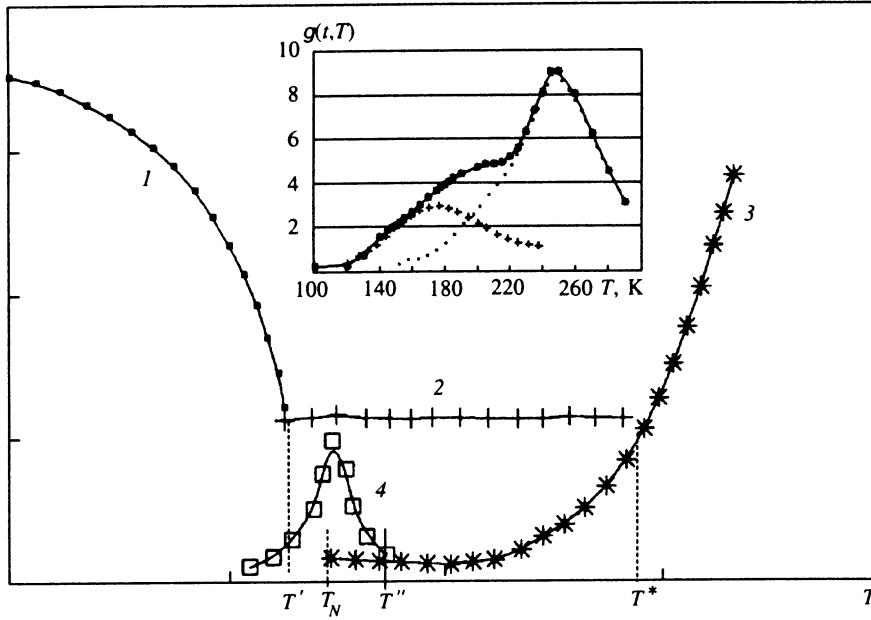
$\Delta\omega, \gamma$

FIG. 6. Schematic temperature dependence of the natural frequencies (curves *1* and *2*) and the damping (curves *3* and *4*) of spin-wave excitations in a Eu_2CuO_4 crystal. The inset shows the temperature dependence of the density of states in an orbital glass according to Ref. 13. See the text proper for an explanation.

with correlation radii ξ as in (4.14). There are an easy-plane anisotropy and a spin–orbit interaction. We assume $\lambda \gg K_a$, and that Hamiltonian (5.1) reduces as a result to the Hamiltonian discussed in Ref. 13:

$$H = \sum_{ij} JS_iS_j + \lambda \sum_i S_i^z \sigma_i^z. \tag{5.4}$$

In second-order perturbation theory in the parameter λ/J we find an effective Hamiltonian for σ_i^z:

$$H_{\text{eff}}^\sigma = \lambda \sum_i \langle S_i^z \rangle \sigma_i^z + \frac{\lambda^2}{J}$$

$$\times \sum_{ij} (-1)^{n_i+n_j} \langle \Omega_i^z \Omega_j^z \rangle \sigma_i^z \sigma_j^z. \tag{5.5}$$

Here $S_i^\alpha = (-1)^{n_i} \Omega_i^\alpha$, with $n_i = 0$ or 1, depending on the particular sublattice to which the given site belongs.

According to Ref. 6, for an antiferromagnet of dimensionality D we would have

$$\langle \Omega_i \Omega_j \rangle \sim r_{ij}^{(D-1)/2} \exp(-r_{ij}/\xi). \tag{5.6}$$

It was shown in Ref. 13 that at $T > T_N$ an orbital-glass states arises in Eu_2CuO_4 by virtue of the long-range orbit–orbit interaction (of alternating sign)

$$V_{ij} = (-1)^{n_i+n_j} \lambda^2 / J \langle \Omega_i^z \Omega_j^z \rangle,$$

which is described by the second term in (5.5). A random field $h_i^s = \lambda \langle \sigma_i^z \rangle$ arises in the spin subsystem in this case. This random field may be stronger than the easy-plane anisotropy. The anisotropy due to the random field h_i^s is an easy-axis anisotropy. As a result, the temperature at which the orbital-glass state arises in the orbital subsystem is simultaneously the temperature at which the spin anisotropy changes sign.

However, the proposed description of the state of the crystal is inconsistent with experiment. Specifically, in this description the orbital-glass state and the change in the sign of the anisotropy should occur at $T > T_N$ (150–160 K), while experiment shows that the corresponding temperature is $T' \approx 120$ K. To clarify this situation, we examine the state of the crystal at $T < T_N$.

We assume that at $T < T_N$ we have 3D antiferromagnetic long-range order with spins lying in the ab plane. In this case we have $\langle S_i^z \rangle = 0$, but there are isotropic 3D antiferromagnetic spin fluctuations, and the interaction V_{ij}, which is responsible for the onset of the orbital-glass state, is nonzero. At $T \ll T_N$, however, the correlation radius $\xi = a[|T - T_N|/T_N]^{-0.7}$ of the 3D antiferromagnetic spin fluctuations is on the order of the lattice constant. It was shown in Ref. 13 that a necessary condition for the onset of an orbital-glass state is that the interaction V_{ij} be long-range.

In a 3D critical region, the value of ξ^{3D} is considerably higher. As a result, at some temperature $T' < T_N$ the interaction V_{ij} becomes of sufficiently long-range that an orbital-glass state can arise. With a subsequent increase in temperature, in a transition from a 3D critical region to a 2D state, we have $\xi^{2D} \gg \xi^{3D}$ [compare (4.14) and (4.11)], and the orbital-glass state persists in the 2D region up to high temperatures.

We thus assume that an orbital-glass state can arise even in the 3D critical region, by virtue of 3D antiferromagnetic spin fluctuations, if the correlation radius ξ^{3D} is sufficiently large. The temperature dependence of the density of states of the orbital glass, found in Ref. 13 and shown in the inset in Fig. 6, does indeed have two maxima: a comparatively small one at $T \approx T_N$ and an absolute one at $T \approx 250$ K. An easy-axis anisotropy due to the random field h_i^s prevails over the entire temperature range in which the orbital-glass state exists.

We also note that some structural features characteristic of structural phase transitions in crystals have been observed at $T' \approx 120$ K in the temperature dependence of the dielectric constant (see Fig. 3). We believe that the change in sign of

the spin anisotropy and the onset of an orbital-glass state at $T \geqslant 120$ K are accompanied by structural distortions in the lattice without a change in the space group of the crystal. In other words, we believe that an isostructural phase transition occurs.

Returning to the intrinsic excitation spectra of the Eu_2CuO_4 crystal for the entire temperature range, we show in Fig. 6 the gross temperature dependence of the natural frequencies and the damping. At $T < T'$ there is 3D antiferromagnetic long-range order, and an easy-plane anisotropy is predominant. Along the c axis of the crystal there is a gap $\Delta\omega^c_{AFMR}$ in the spectrum of spin waves (an antiferromagnetic resonance; curve 1 in Fig. 6):

$$\Delta\omega^c_{AFMR} = \sqrt{T^{2D}_{mf}T_a}. \tag{5.7}$$

There is gapless branch of an antiferromagnetic resonance in the easy plane. If we take the magnitude of the easy-plane anisotropy to be $T_a \sim 0.1$ K (a typical value for crystals of this type), we find that the value of $\Delta\omega^c_{AFMR}$ at $T=0$ is on the order of 400 GHz. As $T \to T_N$, the gap vanishes ($\Delta\omega^c_{AFMR} \to 0$), in accordance with the temperature dependence of the antiferromagnetic order parameter. At $T \geqslant T' \approx 120$ K, well-defined ferromagnetic spin-wave excitations with a frequency $\omega_0 = cq_a$ arise in the crystal (curve 2 in Fig. 6). In our experiments for the c axis of the crystal, we see a transition region from an antiferromagnetic resonance $\Delta\omega^c_{AFMR}$ to uniform, well-defined, ferromagnetic spin-wave excitations with a frequency $\omega_0 \approx 2\times10^{11}$ Hz. If we take the spin-wave velocity to be $c \approx 0.4\times10^6$ cm/s (as in Refs. 2–4 for La_2CuO_4), we can calculate ξ_a; we find $\sim 200a$. Using (4.14) and this value of ξ_a, we can estimate the magnitude of the easy-axis anisotropy to be ~ 250 K.

In the ab plane, in which there is essentially no anisotropy, the frequency of the antiferromagnetic resonance is close to zero at $T < T_N$. For this plane, there are no uniform, well-defined, ferromagnetic spin-wave excitations. There is only a diffuse mode with a relaxation frequency $\gamma \approx c\xi^{-1}$ of the antiferromagnetic order parameter (curve 3 in Fig. 6). In the exchange approximation, this relaxation frequency is the same for both orientations of the crystal. As a result, a 3D critical region is manifested near T_N in the $h \perp c$ orientation: we see maxima of χ'_{mpl} and χ''_{mpl} near 150 K (Fig. 1). The corresponding relaxation frequency for the 3D critical region is shown by curve 4 in Fig. 6. It can be seen from Fig. 1 that the temperature $T'=120$ K is in the 3D critical region and that the values of the susceptibility χ_{mpl} are fairly large at $T=T'$. In the planar orientation, we see structural features in the temperature dependence of χ'_{mpl} and χ''_{mpl} at a temperature $T=T'' \approx 190$–200 K, which we link with the point of the crossover (T'' in Fig. 6) from 3D critical fluctuations to 2D antiferromagnetic spin fluctuations. In the ab plane at $T > T''$ there are only diffuse modes, which can be described by independent relaxers as follows:

$$\chi' = \chi_0 \frac{1}{1+(\omega\tau)^2}, \quad \chi'' = \chi_0 \frac{\omega\tau}{1+(\omega\tau)^2}, \tag{5.8}$$

where τ is the relaxation time. If $\omega\tau \ll 1$ (and this condition holds in our case, since we have $\omega \approx \omega_0$ for a well-defined mode along the c axis, and the damping is identical for the

two orientations), then we have $\chi' \approx \chi_0$ and $\chi'' \approx \omega\tau\chi_0$. In other words, χ' is independent of the temperature, and we have $\chi'' \ll \chi'$, in agreement with experiment.

It can be seen from an analysis of Fig. 6 that a situation with well-defined uniform spin-wave excitations is not common to all crystals of the R_2CuO_4 or $YBa_2Cu_3O_{6+\delta}$ types. The temperature-independent size of the gap of ferromagnetic spin-wave excitations is essentially determined by the magnitude of the anisotropy, since the velocities of spin waves can be assumed to be approximately the same for all crystals of the R_2CuO_4 type. In the exchange approximation, we can also assume that the relaxation frequency γ increases exponentially with the temperature for this entire class of crystals. Whether well-defined uniform ferromagnetic spin-wave excitations can exist will depend on the relation between T_N and the anisotropy: the lower T_N and the larger the anisotropy, the wider the temperature range over which well-defined ferromagnetic spin-wave excitations with $q=0$ exist.

We now return to the question of the value of T_N for Eu_2CuO_4 crystals. As we pointed out in the Introduction, opinion in the literature is divided on the value of T_N, which has been found in different experiments [$T_N = 150$–160 K (Refs. 9 and 10) and $T_N = 250$–270 K (Refs. 11 and 12)]. In Ref. 10, a value $T_N \approx$ K was found by the Mössbauer-effect method for Eu_2CuO_4 crystals lightly doped with Co^{2+} ions, which assume Cu^{2+} sites in the lattice. A study was made of the temperature dependence of the intensities of the lines of the hyperfine lines which arise at $T \leqslant T_N$. The conversion of these lines into a paramagnetic doublet at $T \approx T_N$ was also studied.

In a study of the static susceptibility χ_0 of a Eu_2CuO_4 crystal,[9] the temperature dependence of χ_0 in the plane perpendicular to the c axis (χ_{0pl}) was found. It has the same shape as the temperature dependence of the intensity of the [1/2, 1/2, 0] Bragg antiferromagnetic peak in Ref. 12. At $T \approx 150$ K, there is an abrupt decrease in χ_{0pl}, and the intensities of the [1/2, 1/2, 0] Bragg peak amount to about 10–15% of the value at $T=4.2$ K. Later on, at $T > 150$ K, we observe a linear decrease in χ_{0pl} without any structural feature at $T \approx 270$ K. The subsequent decrease in the intensity of the Bragg peak accelerates as we approach $T \approx 270$ K, which was taken to be T_N in Ref. 12. A fairly sharp decrease in intensity of the Bragg peak was also found in Ref. 11, first at $T \approx 150$ K and then at $T \approx 250$ K.

A discussion of the experimental results of this study showed that the situation can be understood only if we adopt a value $T_N \approx 150$–160 K.

In the integrated-intensity method on the two-crystal diffractometer in Ref. 12 it was the total intensity from the 3D antiferromagnetic [1/2, 1/2, 0] Bragg peak and from 2D antiferromagnetic correlated regions at $T \geqslant T_N$ which was measured, in our opinion. We know (Ref. 5, for example) that the intensity of Bragg elastic scattering is proportional to $\langle S_z \rangle^2$ and vanishes as $T \to T_N$. The strong intensity from Bragg scattering and from scattering by 2D antiferromagnetic correlated regions, on the other hand, is proportional to $S(S+1) \approx 1$. Since we have $\langle S_z \rangle \approx (0.35-0.40)\mu_B$ (where μ_B is the Bohr magneton) in R_2CuO_4 crystals,[2-5] the contribution from elastic Bragg scattering is ≈ 10–15% of the total contribu-

tion. A jump of just this magnitude was observed in the scattering intensity at $T \approx 150$ K in Ref. 12.

At $T > 150$ K, the scattering near the Bragg peak is due primarily to scattering by 2D antiferromagnetic correlated regions with a scale ξ. At temperatures at which the damping of the antiferromagnetic order parameter is slight ($\gamma \propto \xi^{-1}$), the scattering by 2D antiferromagnetic correlated regions is quasielastic. As the temperature is raised, and the damping γ exceeds the values of the natural frequencies of well-defined spin-wave excitations in 2D antiferromagnetic correlated regions, the scattering by them becomes diffuse. Using Eqs. (4.14) and (4.18), along with the experimental values of ω_0 and ξ_a^{2D}, we find that ω_0 and γ become comparable in magnitude at a temperature ≈ 250 K (the temperature T^* in Fig. 6).

No data regarding an analysis of the scattering geometry at $T > 150$ K were reported in Ref. 12. At these temperatures, the jump in the intensity of Bragg antiferromagnetic peak has already occurred. No distinction was made among the contributions of the total intensity from the 3D elastic Bragg peak and the 2D antiferromagnetic correlated regions. Accordingly, we do not believe that it is possible to draw a definitive conclusion regarding the value of T_N for Eu_2CuO_4 on the basis of the data of Refs. 11 and 12.

In summary, uniform ($q = 0$), well-defined, ferromagnetic spin-wave excitations have been observed experimentally in this study over a broad temperature range, including the region $T > T_N$, in the stoichiometric dielectric crystal Eu_2CuO_4 in the absence of a static external magnetic field. These excitations essentially constitute an antiferromagnetic resonance in a critical temperature region and a gap in the spectrum of spin-wave excitations at $T > T_N$.

It has been shown here that incorporating an anisotropy of a certain symmetry and magnitude leads to the possible existence of uniform, well-defined ferro and antiferromagnetic spin-wave excitations, which are usually characteristic of the hydrodynamic region, but which are realized in the critical region under the conditions $a \ll \xi_a \ll \xi$.

Taking account of the specific interactions characteristic of the Eu_2CuO_4 crystal, we have constructed a phase state diagram of the crystal over a broad temperature range. This diagram explains the observed experimental data.

*B. P. Konstantinov St. Petersburg Institute of Nuclear Physics, Russian Academy of Sciences, 188350 St. Petersburg, Russia

[1] J. V. Tranquada, S. Heald, and S. Moodenbaugh, Phys. Rev. B **36**, 8401 (1988).
[2] Y. Endoh, K. Yamada, R. J. Birgeneau et al., Phys. Rev. B **37**, 7443 (1988).
[3] K. Yamada, K. Kakurai, Y. Endoh et al., Phys. Rev. B **40**, 4557 (1989).
[4] J. M. Tranquada, G. Shirane, B. Keimer et al., Phys. Rev. B **40**, 4503 (1989).
[5] O. S. Shamoto, M. Sato, J. M. Tranquada et al., Phys. Rev. B **48**, 13817 (1993).
[6] S. Chacravarty, B. Halperin, and D. Nelson, Phys. Rev. B **39**, 2344 (1989).
[7] S. Tyc, B. Halperin, and S. Chacravarty, Phys. Rev. Lett. **62**, 835 (1989).
[8] E. Manousakis, Rev. Mod. Phys. **63**, 1 (1991).
[9] A. V. Babinskiĭ, E. I. Golovenchits, N. V. Morozov et al., Fiz. Tverd. Tela (Leningrad) **34**, 60 (1992) [Sov. Phys. Solid State **34**, 31 (1992)].
[10] S. Jha, D. Suyanto, R. Hogg et al., Hyperfine Interact. **61**, 1143 (1990).
[11] A. G. Gukasov, S. Yu. Kokovin, V. P. Plakhty et al., Physica B **180–181**, 455 (1992).
[12] T. Chatopadhyaya, J. W. Lynn, N. Rosov et al., Phys. Rev. B **49**, 9944 (1994).
[13] A. V. Babinskiĭ, S. L. Ginzburg, E. I. Golovenchits, and V. A. Sanina, JETP Lett. **57**, 289 (1993).
[14] B. I. Halperin and P. C. Hohenberg, Phys. Rev. **177**, 952 (1969).
[15] A. G. Gurevich, Microwave Ferrites [in Russian], Fizmatgiz, Moscow (1960).
[16] L. D. Landau and E. M. Lifshitz, Electrodynamics of Continuous Media, Pergamon, Oxford (1984).
[17] A. S. Borovik-Romanov and V. I. Ozhogin, Zh. Éksp. Teor. Fiz. **39**, 27 (1960) [Sov. Phys. JETP **12**, 18 (1961)].
[18] J. Friedel, J. Phys (Paris) **49**, 1561 (1988).
[19] J. M. Kosterlitz and D. J. Thouless, J. Phys. C **6**, 1181 (1973).

Translated by D. Parsons